












Insights into jet–NLR energetics in PMN J0948+0022

B. Dalla Barba^{1,2,3}, L. Foschini², M. Berton³,
A. Lähteenmäki^{4,5}, M. Tornikoski⁴, E. Sani³, L. Crepaldi^{6,7},
E. Congiu³, G. Venturi^{8,9}, W.J. Hon¹⁰ and A. Vietri^{11,6}

¹ *Università degli studi dell’Insubria, Via Valleggio 11, Como 22100, Italy*

² *Osservatorio Astronomico di Brera, Istituto Nazionale di Astrofisica (INAF), Via E. Bianchi 46, Merate (LC) 23807, Italy*

³ *European Southern Observatory (ESO), Alonso de Córdova 3107, Vitacura Santiago, Chile*

⁴ *Aalto University Metsähovi Radio Observatory, Metsähovintie 114, FI-02540 Kylmälä, Finland*

⁵ *Aalto University Department of Electronics and Nanoengineering, P.O. Box 15500, FI-00076 AALTO, Finland*

⁶ *Dipartimento di Fisica e Astronomia “G. Galilei”, Università degli studi di Padova, Vicolo dell’Osservatorio 3, Padova 35122, Italy*

⁷ *Osservatorio Astronomico di Cagliari, Istituto Nazionale di Astrofisica (INAF), Via della Scienza 5, 09047 Selargius, Italy*

⁸ *Scuola Normale Superiore, Piazza dei Cavalieri 7, Pisa 56126, Italy*

⁹ *Osservatorio Astrofisico di Arcetri, Istituto Nazionale di Astrofisica (INAF), Largo E. Fermi 5, Firenze 50125, Italy*

¹⁰ *School of Physics, University of Melbourne, Parkville, Victoria 3010, Australia*

¹¹ *Osservatorio Astronomico di Padova, Istituto Nazionale di Astrofisica (INAF), Vicolo dell’Osservatorio 5, 35122 Padova, Italy (E-mail: benedetta.dallabarba@inaf.it)*

Received: July 21, 2025; Accepted: November 5, 2025

Abstract. The analysis of the optical spectra of PMN J0948+0022 showed significant variations in the spectral lines that, when combined with the *Fermi* γ –ray light curve and radio observations reported by other authors, were interpreted as the result of interactions between the relativistic jet and the narrow-line region (NLR). In this work, we present order-of-magnitude calculations of the energetics associated with this proposed jet–NLR interaction. We demonstrate that the observed outflows are capable of absorbing a fraction of the jet energy and converting it into kinetic energy. This mechanism provides a natural explanation for the optical spectral variability recorded with the X-shooter

and Multi-Unit Spectroscopic Explorer (MUSE) instruments. Our results support the scenario in which feedback from the relativistic jet can dynamically influence the circumnuclear gas, offering new insights into the coupling between jets and the NLR in γ -ray-emitting narrow-line Seyfert 1 galaxies.

Key words: Seyfert galaxies – individual: PMN J0948+0022 – optical spectroscopy

1. Introduction

Among active galactic nuclei (AGN), narrow-line Seyfert 1 galaxies (NLS1s) represent a peculiar class of objects. NLS1s are spectroscopically classified sources with relatively narrow $H\beta$, faint $[O\ III]\lambda 5007$, and often strong Fe II multiplets (Osterbrock & Pogge, 1985; Goodrich, 1989). The importance of these sources lies in their nature as young or rejuvenated quasars (Mathur, 2000), potentially representing the progenitors of more evolved quasars (Berton et al., 2016, 2017, 2025). A small fraction of NLS1s show relativistic jet emission, which in some cases makes the sources detectable at γ -rays (γ -NLS1s). The first example of such a source is PMN J0948+0022 ($z = 0.585$; Williams et al. 2002; Zhou et al. 2003; Ahn et al. 2012; Foschini et al. 2010). To date, about two dozen γ -NLS1s have been identified (e.g., Foschini et al. 2022), and their number is steadily increasing.

In Dalla Barba et al. (2025) (hereafter referred to as DB25), we analyzed the optical spectral variations of PMN J0948+0022, focusing on the $H\beta$ and $[O\ III]\lambda\lambda 4959, 5007$ emission lines. We detected variability in the $[O\ III]\lambda 5007$ core flux, in its outflow component, and in the outflow velocity. Based on intermediate-resolution ($R = \lambda/\Delta\lambda \sim 6500 - 2500$) X-shooter (2017-12-17) and Multi-Unit Spectroscopic Explorer (MUSE) spectra (between 2022-11-24 and 2023-03-08, the analyzed spectrum combines data from all epochs), we proposed a reclassification of this source from a NLS1 to an intermediate Seyfert, characterized by a composite profile for the Balmer lines. We suggested that the X-shooter and MUSE $H\beta$ profiles are not due to a geometrical effect of partial obscuration, but rather to the interaction of the relativistic jet with the narrow-line region (NLR). This interaction was previously suggested by Doi et al. (2019) from the study of the radio component of the jet. The authors found a jet-shape change at a distance of ~ 100 -400 pc from the center, compatible with our estimate of the distance of the outflow ($D_{out} \sim 130$ -220 pc). From this, we proposed that the jet impacted the outflowing bubble, producing both the observed shape variation of the jet and the release of part of its energy into the surrounding NLR, which in turn generated the observed optical spectral variations.

In this work, we extend the study presented in DB25, focusing on the energetics of the jet-NLR interaction. These are back-of-the-envelope calculations, meant to provide an order-of-magnitude estimate of the process. The paper is organized as follows: Section 2 presents the physical conditions and energetics of

the NLR; Section 3 describes the energetics of the jet from γ -ray and radio data; Section 4 discusses the results and conclusions. Throughout the manuscript we assume a standard Λ CDM cosmology with $H_0=73.3 \text{ km s}^{-1} \text{ Mpc}^{-1}$, $\Omega_m=0.3$, and $\Omega_\Lambda=0.7$ (Riess et al., 2022).

2. NLR and outflow properties

In general, from line ratios such as [O II] and [S II] we can estimate the electron density (n_e) and temperature (T_e) of the gas in the NLR. Given the X-shooter and MUSE spectral coverage, [S II] lines are not present in both PMN J0948+0022 spectra. For this reason, we assumed a typical $T_e \sim 10^4 \text{ K}$ (Osterbrock & Ferland, 2006) and calculated the electron density from the [O II] $\lambda\lambda 3726, 3729$ lines using PyNeb (Luridiana et al., 2013, 2015), a Python tool to compute emission line emissivities from recombination and collisionally excited lines (in our case we used only collisionally excited lines). The [O II] line fluxes from DB25 are reported in Table 2. The results, expressed as the median values obtained from $N=5000$ iterations with initial values inside the error bars of the observed fluxes, are: $n_{e,X} \sim 170 \text{ cm}^{-3}$ and $n_{e,M} \sim 260 \text{ cm}^{-3}$, for the X-shooter and MUSE cases, respectively.

From the calculated n_e and the [O III] $\lambda 5007$ luminosity of the outflow (L_{5007}^{out}), we can estimate the mass of the outflow (M_{out}). The L_{5007}^{out} parameter was obtained from $L_{5007}^{\text{out}} = 4\pi d_L^2 F_{5007}^{\text{out}}$, where d_L is the luminosity distance and F_{5007}^{out} is the observed flux of the outflowing component in [O III] (see again Table 2). M_{out} is then calculated using the relation from Komossa et al. (2018):

$$M_{\text{out}} = 67.4 \times 10^7 \left(\frac{L_{5007}^{\text{out}}}{10^{42} \text{ erg s}^{-1}} \right) \left(\frac{n_e}{100 \text{ cm}^{-3}} \right)^{-1} M_\odot \quad (1)$$

where we re-scaled by a factor 10 the relation to use the [O III] luminosity instead of the $H\beta$ one, as suggested by Komossa et al. (2018). For the two cases, the results are: $M_{\text{out},X} \sim 8.6 \cdot 10^7 M_\odot$ and $M_{\text{out},M} \sim 3.9 \cdot 10^7 M_\odot$.

Following the same reasoning presented in Blustin et al. (2005) and Venturi et al. (2023), the mass outflow rate through a spherical surface of radius r subtended by a solid angle Ω , with covering factor CF , is $\dot{M}_{\text{out}} = \Omega r^2 \rho v_{\text{out}} \cdot CF$. If the outflowing mass M_{out} is contained in a thin shell of radial thickness R_{out} , its volume is approximately $V \simeq \Omega r^2 R_{\text{out}}$ and therefore:

$$\begin{aligned} \dot{M}_{\text{out}} &\sim \Omega r^2 \frac{M_{\text{out}}}{V} v_{\text{out}} \cdot CF \sim \cancel{\Omega} \frac{M_{\text{out}}}{\cancel{\Omega} r^2 R_{\text{out}}} \cancel{r^2} v_{\text{out}} \cdot CF \sim \\ &\sim \frac{M_{\text{out}}}{R_{\text{out}}} v_{\text{out}} \cdot CF \sim \frac{M_{\text{out}}}{D_{\text{out}} \cdot 0.1} v_{\text{out}} \cdot 0.1 \end{aligned} \quad (2)$$

assuming roughly constant density and velocity across the shell, we have adopted a reference covering factor $CF \sim 0.1$ and an outflow distance from the center

of $D_{out} \sim R_{out}/0.1 \sim 173$ pc (see the mean value reported in Table 2). In the D_{out} expression, we have further assumed a conical shape for the jet. Finally, the kinetic power of the outflow is:

$$\dot{E}_{kin} = \frac{1}{2} \dot{M}_{out} v_{out}^2 = P_{out} \quad (3)$$

The resulting estimates for the two cases are $P_{out,X} \sim 8.8 \cdot 10^{42}$ erg s⁻¹ and $P_{out,M} \sim 14 \cdot 10^{42}$ erg s⁻¹.

If we instead assume electron temperatures in the range $T_e = (5 - 20) \cdot 10^4$ K (Osterbrock & Ferland, 2006), the resulting densities are $n_{e,X} \sim 120 - 210$ cm⁻³ and $n_{e,M} \sim 190 - 320$ cm⁻³. The corresponding outflow powers are $P_{out,X} \sim (7.0 - 12) \cdot 10^{42}$ erg s⁻¹ and $P_{out,M} \sim (12 - 19) \cdot 10^{42}$ erg s⁻¹. In all cases, these variations do not affect the conclusions.

3. Jet power

3.1. γ -ray component

We calculated the radiative power of the jet ($P_{\gamma,rad}$) from *Fermi* data obtained in epochs nearly simultaneous with the X-shooter and MUSE observations. For X-shooter, we used the photon flux from 2017-12-30, while for MUSE we calculated the mean value of the *Fermi* datapoints over the interval 2022-12-04 to 2023-02-02. We multiplied the photon flux (F_γ , reported in Table 2) by the photon mean energy, using 1 GeV as reference for the conversion, and then obtained the flux in erg s⁻¹ cm⁻². We calculated the corresponding luminosity (L_γ) using:

$$L_\gamma = 4\pi d_L^2 \frac{F_\gamma}{(1+z)^{1-\alpha_\gamma}} \quad (4)$$

where α_γ is the spectral index in the γ -rays obtained from the *Fermi* light-curve repository (see Table 2). With the luminosity, we then calculated $P_{\gamma,rad}$ using the equation from Maraschi & Tavecchio (2003):

$$P_{\gamma,rad} = \Gamma^2 \frac{L_\gamma}{\delta^4} \quad (5)$$

where Γ is the bulk Lorentz factor and δ the corresponding Doppler factor. As reported in Table 2, we can assume two possible values for these quantities, which lead to four different results. Here we report only the two mean values: $P_{\gamma,rad,X} \sim 2.5 \times 10^{44}$ erg s⁻¹ and $P_{\gamma,rad,M} \sim 2.4 \times 10^{44}$ erg s⁻¹. Finally, we assume that the kinetic power is ten times the radiative one, see Table 1 for $P_{\gamma,kin}$.

3.2. Radio component

For the radio component, we can use the relation presented in Foschini et al. (2024) to obtain kinetic ($P_{radio,kin}$) power of the jet:

$$P_{radio,kin} = 3.9 \times 10^{44} \left(\frac{S_\nu d_L^2}{1+z} \right)^{\frac{12}{17}} \text{ erg s}^{-1} \quad (6)$$

where S_ν is the radio flux density in Jy (see Table 2). The radio data were taken from the monitoring of the source performed by the Metsähovi Radio Observatory at 37 GHz. For the X-shooter epoch we used the flux averaged between 2017-12-06 and 2017-12-22, and for the MUSE epochs the flux averaged between 2022-12-02 and 2023-03-06. The results are: $P_{radio,kin,X} \sim 4.8 \cdot 10^{44} \text{ erg s}^{-1}$ and $P_{radio,kin,M} \sim 7.3 \cdot 10^{44} \text{ erg s}^{-1}$.

4. Discussion and conclusions

From the values reported in reported Table 1, we can compare the kinetic powers of the outflow with those of the jet in its γ -ray and radio components. Specifically, we find that the outflow kinetic power constitutes a small but non-negligible fraction of the jet power in both epochs. The respective ratios, listed in Table 1, indicate that approximately 0.35%-1.9% of the jet power has been deposited into the outflow in both epochs. This further supports the scenario proposed in DB25, where we suggested that the observed variations in the outflow properties (in terms of flux and velocity) could result from the interaction between the jet and the NLR. In turn, these variations in the outflow kinetic power would likely be driven by changes in the jet state and energetics.

Table 1. Summary of the kinetic powers and of the ratios between the outflow power and the γ -ray and radio jet powers ($R_{out,\gamma}$ and $R_{out,radio}$, respectively).

Epoch	P_{out} [erg s ⁻¹]	$P_{\gamma,kin}$ [erg s ⁻¹]	$P_{radio,kin}$ [erg s ⁻¹]	$R_{out,\gamma}$	$R_{out,radio}$
X-shooter	$8.8 \cdot 10^{42}$	$2.5 \cdot 10^{45}$	$4.8 \cdot 10^{44}$	0.35%	0.55%
MUSE	$14 \cdot 10^{42}$	$2.4 \cdot 10^{45}$	$7.3 \cdot 10^{44}$	0.58%	1.9%

These results support a scenario in which the relativistic jet deposits part of its energy into the surrounding environment – specifically, the NLR – producing the observed variations in the optical spectra, particularly in the [O III] $\lambda 5007$ outflow properties. This hypothesis is also supported by the radio study of Doi et al. 2019. Our optical spectroscopic analysis (DB25) provides a crucial link

between these radio observations and the optical data, linking changes in jet morphology with the variability observed in both the optical band and the γ -rays. The order-of-magnitude calculations presented here provide further evidence that, from an energetic perspective, the jet-NLR interaction can account for the observed optical spectral variations. Together, these findings reinforce the notion that the interplay between the relativistic jet and the circumnuclear gas significantly influences both the kinematics and energetics of the NLR in γ -NLS1 galaxies. Similar results have been reported by other authors, who observed variability in spectral features associated with jet activity. Examples include variable Mg II lines (e.g., León-Tavares et al. 2013; Berton et al. 2018; Yang et al. 2020) and changes in the broad H β component (Hon et al., 2023).

In conclusion, this analysis, combined with the results reported in DB25, underscores the importance of a multi-wavelength approach to the study of AGN, particularly for jetted sources. The combination of multi-epoch optical spectroscopy, radio observations, and γ -ray monitoring is essential for a better understanding of the mechanisms driving the interplay between jet emission and the AGN environment.

Acknowledgements. B.D.B. thank the organizers of the 15th Serbian Conference on Spectral Line Shapes in Astrophysics for the contributed talk. G.V. acknowledges support from the European Union (ERC, WINGS, 101040227). This publication makes use of data obtained at Metsähovi Radio Observatory, operated by Aalto University in Finland.

References

- Abdollahi, S., Ajello, M., Baldini, L., et al., The Fermi-LAT Lightcurve Repository. 2023, *Astrophysical Journal, Supplement*, **265**, 31, DOI:10.3847/1538-4365/acbb6a
- Ahn, C. P., Alexandroff, R., Allende Prieto, C., et al., The Ninth Data Release of the Sloan Digital Sky Survey: First Spectroscopic Data from the SDSS-III Baryon Oscillation Spectroscopic Survey. 2012, *Astrophysical Journal, Supplement*, **203**, 21, DOI:10.1088/0067-0049/203/2/21
- Berton, M., Foschini, L., Caccianiga, A., et al., An orientation-based unification of young jetted active galactic nuclei: the case of 3C 286. 2017, *Frontiers in Astronomy and Space Sciences*, **4**, 8, DOI:10.3389/fspas.2017.00008
- Berton, M., Foschini, L., Ciroi, S., et al., [O III] line properties in two samples of radio-emitting narrow-line Seyfert 1 galaxies. 2016, *Astronomy and Astrophysics*, **591**, A88, DOI:10.1051/0004-6361/201527056
- Berton, M., Järvelä, E., Tortosa, A., & Mazzucchelli, C., How similar are narrow-line Seyfert 1 galaxies and high-z type 1 AGN? 2025, *arXiv e-prints*, arXiv:2509.03576, DOI:10.48550/arXiv.2509.03576
- Berton, M., Liao, N. H., La Mura, G., et al., The flat-spectrum radio quasar 3C 345 from the high to the low emission state. 2018, *Astronomy and Astrophysics*, **614**, A148, DOI:10.1051/0004-6361/201731625

- Blustin, A. J., Page, M. J., Fuerst, S. V., Branduardi-Raymont, G., & Ashton, C. E., The nature and origin of Seyfert warm absorbers. 2005, *Astronomy and Astrophysics*, **431**, 111, DOI:10.1051/0004-6361:20041775
- Dalla Barba, B., Berton, M., Foschini, L., et al., Interaction of the relativistic jet and the narrow-line region of PMN J0948+0022. 2025, *Astronomy and Astrophysics*, **698**, A320, DOI:10.1051/0004-6361/202452421
- Doi, A., Nakahara, S., Nakamura, M., et al., Radio jet structures at ~ 100 pc and larger scales of the γ -ray-emitting narrow-line Seyfert 1 galaxy PMN J0948+0022. 2019, *Monthly Notices of the RAS*, **487**, 640, DOI:10.1093/mnras/stz1290
- Foschini, L., Angelakis, E., Fuhrmann, L., et al., Radio-to- γ -ray monitoring of the narrow-line Seyfert 1 galaxy PMN J0948 + 0022 from 2008 to 2011. 2012, *Astronomy and Astrophysics*, **548**, A106, DOI:10.1051/0004-6361/201220225
- Foschini, L., Dalla Barba, B., Tornikoski, M., et al., The Power of Relativistic Jets: A Comparative Study. 2024, *Universe*, **10**, 156, DOI:10.3390/universe10040156
- Foschini, L., Fermi/Lat Collaboration, Ghisellini, G., et al., Fermi/LAT Discovery of Gamma-Ray Emission from a Relativistic Jet in the Narrow-Line Seyfert 1 Quasar PMN J0948+0022. 2010, in *Astronomical Society of the Pacific Conference Series*, Vol. **427**, *Accretion and Ejection in AGN: a Global View*, ed. L. Maraschi, G. Ghisellini, R. Della Ceca, & F. Tavecchio, 243–248
- Foschini, L., Lister, M. L., Andernach, H., et al., A New Sample of Gamma-Ray Emitting Jetted Active Galactic Nuclei. 2022, *Universe*, **8**, 587, DOI:10.3390/universe8110587
- Goodrich, R. W., Spectropolarimetry of “Narrow-Line” Seyfert 1 Galaxies. 1989, *Astrophysical Journal*, **342**, 224, DOI:10.1086/167586
- Hon, W., Berton, M., Sani, E., et al., A redshifted excess in the broad emission lines after the flare of the γ -ray narrow-line Seyfert 1 PKS 2004–447. 2023, *Astronomy and Astrophysics*, **672**, L14, DOI:10.1051/0004-6361/202245184
- Komossa, S., Xu, D. W., & Wagner, A. Y., Extreme gaseous outflows in radio-loud narrow-line Seyfert 1 galaxies. 2018, *Monthly Notices of the RAS*, **477**, 5115, DOI:10.1093/mnras/sty901
- León-Tavares, J., Chavushyan, V., Patiño-Álvarez, V., et al., Flare-like Variability of the Mg II $\lambda 2800$ Emission Line in the Γ -Ray Blazar 3C 454.3. 2013, *Astrophysical Journal, Letters*, **763**, L36, DOI:10.1088/2041-8205/763/2/L36
- Luridiana, V., Morisset, C., & Shaw, R. A. 2013, PyNeb: Analysis of emission lines, *Astrophysics Source Code Library*, record ascl:1304.021
- Luridiana, V., Morisset, C., & Shaw, R. A., PyNeb: a new tool for analyzing emission lines. I. Code description and validation of results. 2015, *Astronomy and Astrophysics*, **573**, A42, DOI:10.1051/0004-6361/201323152
- Maraschi, L. & Tavecchio, F., The Jet-Disk Connection and Blazar Unification. 2003, *Astrophysical Journal*, **593**, 667, DOI:10.1086/342118

- Mathur, S., Narrow-line Seyfert 1 galaxies and the evolution of galaxies and active galaxies. 2000, *Monthly Notices of the RAS*, **314**, L17, DOI:10.1046/j.1365-8711.2000.03530.x
- Osterbrock, D. E. & Ferland, G. J. 2006, *Astrophysics of gaseous nebulae and active galactic nuclei* (University Science Books)
- Osterbrock, D. E. & Pogge, R. W., The spectra of narrow-line Seyfert 1 galaxies. 1985, *Astrophysical Journal*, **297**, 166, DOI:10.1086/163513
- Riess, A. G., Yuan, W., Macri, L. M., et al., A Comprehensive Measurement of the Local Value of the Hubble Constant with $1 \text{ km s}^{-1} \text{ Mpc}^{-1}$ Uncertainty from the Hubble Space Telescope and the SH0ES Team. 2022, *Astrophysical Journal, Letters*, **934**, L7, DOI:10.3847/2041-8213/ac5c5b
- Venturi, G., Treister, E., Finlez, C., et al., Complex AGN feedback in the Teacup galaxy. A powerful ionised galactic outflow, jet-ISM interaction, and evidence for AGN-triggered star formation in a giant bubble. 2023, *Astronomy and Astrophysics*, **678**, A127, DOI:10.1051/0004-6361/202347375
- Williams, R. J., Pogge, R. W., & Mathur, S., Narrow-line Seyfert 1 Galaxies from the Sloan Digital Sky Survey Early Data Release. 2002, *Astronomical Journal*, **124**, 3042, DOI:10.1086/344765
- Yang, Q., Shen, Y., Chen, Y.-C., et al., Spectral variability of a sample of extreme variability quasars and implications for the Mg II broad-line region. 2020, *Monthly Notices of the RAS*, **493**, 5773, DOI:10.1093/mnras/staa645
- Zhou, H.-Y., Wang, T.-G., Dong, X.-B., Zhou, Y.-Y., & Li, C., SDSS J094857.3+002225: A Very Radio Loud, Narrow-Line Quasar with Relativistic Jets? 2003, *Astrophysical Journal*, **584**, 147, DOI:10.1086/345523

A. Useful quantities

Table 2. List of the quantities involved in the calculations. References: *FLCR*) *Fermi* light-curve repository (Abdollahi et al., 2023), F12) Foschini et al. (2012), *Mets*) Metsähovi Radio Observatory data.

Quantity	Symbol(s)	Value(s)	Units	Reference
Luminosity distance	d_L	3.2	Gpc	Redshift
Outflow distance	D_{out}	$130/220 \rightarrow 170$	pc	DB25
X-shooter [O II] λ 3726 flux	$F_{3726,X}$	$(3.0 \pm 0.6) \times 10^{-17}$	erg s $^{-1}$ cm 2	DB25
X-shooter [O II] λ 3729 flux	$F_{3729,X}$	$(4.3 \pm 0.4) \times 10^{-17}$	erg s $^{-1}$ cm 2	DB25
MUSE [O II] λ 3726 flux	$F_{3726,M}$	$(8.4 \pm 0.6) \times 10^{-17}$	erg s $^{-1}$ cm 2	DB25
MUSE [O II] λ 3729 flux	$F_{3729,M}$	$(9.9 \pm 0.6) \times 10^{-17}$	erg s $^{-1}$ cm 2	DB25
<i>Fermi</i> flux in the X-shooter epoch	$F_{\gamma,X}$	4.0×10^{-8}	ph s $^{-1}$ cm 2	<i>FLCR</i>
<i>Fermi</i> flux in the MUSE epochs	$F_{\gamma,M}$	3.8×10^{-8}	ph s $^{-1}$ cm 2	<i>FLCR</i>
X-shooter [O III] λ 5007 outflow luminosity	$L_{5007,X}^{out}$	2.1×10^{41}	erg s $^{-1}$	DB25
MUSE [O III] λ 5007 outflow luminosity	$L_{5007,M}^{out}$	1.5×10^{41}	erg s $^{-1}$	DB25
Radio flux density close to the X-shooter epoch	$S_{\nu,X}$	0.20	Jy	<i>Mets</i>
Radio flux density close to the MUSE epochs	$S_{\nu,M}$	0.37	Jy	<i>Mets</i>
X-shooter [O III] λ 5007 outflow velocity	$v_{out,X}$	380	km s $^{-1}$	DB25
MUSE [O III] λ 5007 outflow velocity	$v_{out,M}$	580	km s $^{-1}$	DB25
<i>Fermi</i> spectral index	α_γ	2.5	-	<i>FLCR</i>
Bulk Lorentz factor (two cases)	$\Gamma_{1,2}$	11/16	-	F12
Doppler factor (two cases)	$\delta_{1,2}$	17/19	-	F12